

# Lawrence Berkeley National Laboratory

## Recent Work

### Title

SOLUBLE THEORY OF NONLINEAR BEAM-PLASMA INTERACTION

### Permalink

<https://escholarship.org/uc/item/9bd9w0jj>

### Author

Mynick, Harry E.

### Publication Date

1977-04-01

RECEIVED  
UNIVERSITY OF CALIFORNIA  
BERKELEY LABORATORY

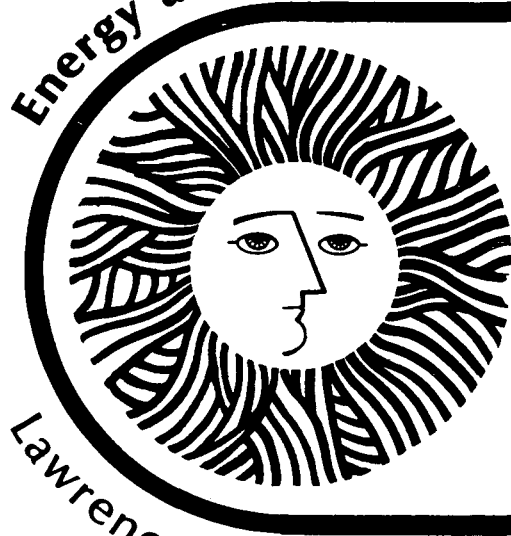
MAR 30 1978

LIBRARY AND  
DOCUMENTS SECTION

**For Reference**

Not to be taken from this room

**Energy and Environment Division**



Soluble Theory Of Nonlinear  
Beam-Plasma Interaction

*Harry E. Mynick and Allan N. Kaufman*

April 28, 1977

Lawrence Berkeley Laboratory University of California/Berkeley

Prepared for the U.S. Department of Energy under Contract No. W-7405-ENG-48

000004801/80

## **DISCLAIMER**

This document was prepared as an account of work sponsored by the United States Government. While this document is believed to contain correct information, neither the United States Government nor any agency thereof, nor the Regents of the University of California, nor any of their employees, makes any warranty, express or implied, or assumes any legal responsibility for the accuracy, completeness, or usefulness of any information, apparatus, product, or process disclosed, or represents that its use would not infringe privately owned rights. Reference herein to any specific commercial product, process, or service by its trade name, trademark, manufacturer, or otherwise, does not necessarily constitute or imply its endorsement, recommendation, or favoring by the United States Government or any agency thereof, or the Regents of the University of California. The views and opinions of authors expressed herein do not necessarily state or reflect those of the United States Government or any agency thereof or the Regents of the University of California.

## SOLUBLE THEORY OF NONLINEAR BEAM-PLASMA INTERACTION\*

Harry E. Mynick and Allan N. Kaufman

Department of Physics and Lawrence Berkeley Laboratory  
University of California, Berkeley, California 94720

## ABSTRACT

A soluble theory of the post-saturation portion of a beam-plasma interaction is developed, concentrating on explaining the results of O'Neil, Winfrey, and Malmberg. Analytic progress is made possible by applying a certain constraint-procedure, characterized by the "rotating-bar" approximation, to a Hamiltonian formulation of the problem. The procedure yields, from the original  $N$ -particle Hamiltonian  $H$ , and new, reduced Hamiltonian  $H$ , which has only two particle-related degrees of freedom, and which maintains the conservation laws of energy and momentum possessed by  $H$ . The equations of motion coming from  $H$  still describe the self-consistent interaction of a mode of the plasma with the beam particles, as opposed to previous work, and, because of the great reduction in the number of degrees of freedom, explicit expressions for the nonlinear frequency shift, and growth rate, of the mode can be obtained which are in very good agreement with the simulation results of O'Neil et al.

## I. INTRODUCTION

A beam injected into a dielectric medium (such as a plasma) at an initial velocity nearly equal to the phase velocity of a linear normal mode of the medium, can destabilize the mode, causing its wave amplitude to grow and the wave phase velocity to shift from its linear, unperturbed value. We can unify these two ideas in terms of a complex frequency shift  $\delta\omega = \delta\omega_R + i\gamma$ , where the (real) frequency shift  $\delta\omega_R$  corresponds to a shift in the phase velocity, and  $\gamma$  represents growth rate (or damping) of the wave amplitude.

After the wave has grown sufficiently, saturation of the growth occurs due to trapping of the beam particles in the wave troughs. Simulations<sup>1,2</sup> (see Fig. 1) show a characteristic time dependence of  $\gamma(t)$  and  $\delta\omega_R(t)$  for the subsequent nonlinear, post-saturation portion of the beam-plasma interaction. Components at the bounce frequency  $\omega_b$  of the particles in the wave, and at its second harmonic  $2\omega_b$ , are clearly present in the time dependences of  $\delta\omega_R$  and  $\gamma$ .

The problem envisioned here is one in which we have a single wave which is exactly periodic in space, but perturbed from a strictly

78710840000

sinusoidal time dependence by the presence of the beam particles. In Ref. 3, the authors point out that this does not directly correspond to a realistic experimental situation. A more realistic situation to consider is a wave whose time-dependence is strictly periodic, and whose spatial-dependence is perturbed from a sinusoid by the beam particles. In Ref. 3 it is shown, however, that the resultant scaled equations of the temporal or spatial development of the interaction are the same, but with the roles of the spatial and temporal coordinates in the two cases interchanged.

Related to the beam-plasma interaction are problems involving the time-independent interaction of a plasma wave with resonant particles in the plasma distribution itself. Many studies, including experiments, simulations, and analytic work, have been done on both of these types of resonant particle-wave interactions.<sup>1-9</sup> The analyses of these studies use momentum and energy conservation ideas to conclude that the growth rate  $\gamma$  should oscillate at  $\omega_b$ , while the frequency shift  $\delta\omega_R$  should oscillate at  $2\omega_b$ . The analyses generally use a "frozen wave" model for this line of argument, i. e., they view the wave amplitude and phase velocity as constant on the time scale of the particle bounce time. These analyses therefore suffer from a lack of self-consistency.

In this paper we shall concentrate on the work of O'Neil, et al., although the more general applicability to these other related works should be clear. Those authors reach the previously mentioned general expectations for the time dependence of  $\delta\omega_R$  and  $\gamma$ : that  $\gamma(t)$  oscillates at  $\omega_b$ , while  $\delta\omega_R(t)$  oscillates at  $2\omega_b$ . Inspection of their results, reproduced here in Fig. 1, however, indicates that this is not the whole story. The shape of  $\gamma(t)$  (dimensionless variable  $\Omega_T$ ) is not a simple sinusoid, but rather a sawtoothed shape, rising faster than it falls. Also,  $\delta\omega_R(t)$  (dimensionless variable  $\Omega_R$ ) is far from a simple sinusoid at twice  $\omega_b$ . It appears rather as a superposition of harmonics having fundamental frequency  $\omega_b$ , and having a substantial component at that fundamental frequency. It displays a pattern of rather deep downward spikes followed by a fairly flat, convex upward portion, this pattern repeating itself about every bounce period. Superposed on this is an additional component at what appears to be  $2\omega_b$ . In addition, there is a specific phase relation between the  $\omega_b$  components of  $\delta\omega_R$  and  $\gamma$ , namely, that the trough bottom in  $\delta\omega_R(t)$  occurs simultaneously with the upward zero-crossing in  $\gamma(t)$ .

In this paper we shall present an analysis of the nonlinear (post-saturation) portion of the problem studied in Ref. 1 which gives explanations for all these features of their results. The analysis is made possible through an approximation (the "rotating-bar model") which allows a reduction of the problem from the  $(N + 1)$  degrees of freedom in the full problem (one wave plus  $N$  particle degrees) to a problem with only three degrees of freedom (one wave plus two particle-related degrees). The key approximation, noted by O'Neil et al. but then not used by them except in a qualitative fashion, is to regard the phase-space trajectories  $\Gamma_j(t) = [x_j(t), v_j(t)]$  ( $j = 1, 2 \dots N$ ) of the particles trapped in a given wave trough as described by an average motion of the particles  $\Gamma_0(t)$ , plus a revolving motion  $\delta\Gamma_j(t)$  of the phase space of the  $j$ th particle position about this  $\Gamma_0(t)$ , where the frequency of revolution  $\omega_r$  is the same for all  $j$ . Lampe and Sprangle<sup>2</sup> also use a rotating-bar idea to obtain estimates for the expected amplitude of variation of  $\gamma(t)$ , however, their bar center and wave amplitude and phase are frozen. The present work formalizes the rotating bar concept and builds it into a self-consistent set of equations of motion. We impose this approximation on a Hamiltonian formulation of the full problem via a reduction procedure, applicable to Hamiltonian or Lagrangian descriptions, which yields a new, reduced-Hamiltonian formulation. In this way we maintain the conservation laws (of energy and momentum) present in the full problem, which are helpful in further simplifying the equations of motion to be solved.

The relative simplicity of the reduced, rotating-bar problem allows us to deal with the particle-wave interaction in a

self-consistent manner. The self-consistent solution gives results not expected from the frozen-wave analysis; an enhancement of the particle bounce frequency over the static wave value, and components in  $\delta\omega_R$  at not just  $2\omega_b$  but also at  $\omega_b$ . The frozen-wave assumption should be valid when either the time scale of variation of the wave phase and amplitude are on a much longer time scale than the particle bounce time, or when the magnitude of variation of the wave is so small as to be negligible. Since it is the bouncing particles themselves which are causing the time-variation of the wave, we know that the former of these conditions is violated. The fact that results are found not predicted from a frozen-wave analysis shows that also the latter of these conditions is not well-satisfied.

The organization of the remainder of the paper is as follows. In Sec. II we set up the full  $N$ -particle problem studied by O'Neil et al., discussing their equations of motion, the initial conditions to be applied to the post-saturation interval of the problem with which we are concerned here, and a Hamiltonian formulation of the problem. In Sec. III we describe the formal reduction procedure we employ to obtain the rotating-bar model in Hamiltonian term. In Sec. IV we obtain solutions of the reduced problem's equations of motion. Sec. V is a presentation of the results obtained, and Sec. VI is a general discussion of our findings, and of the reduction technique.

## II. THE FULL N-PARTICLE PROBLEM

In Part A of this section we shall rederive the equations used in Ref. (1). In the present work, we are chiefly concerned with the post-saturation interval of the interaction's time development, and so in Part B we discuss the specification of

00004801788

initial conditions appropriate to this time interval. Part C casts the problem in a Hamiltonian framework.

(A) Equations of Motion

Following O'Neil et al., we consider a one-dimensional beam-plasma system, where the initial beam velocity  $v_0$  is equal to the linear phase velocity of a normal mode of the plasma in the absence of the beam. As in Ref. 1, we consider only this single mode, assuming that it is the fastest-growing one, and so will dominate the wave spectrum, at least for a few e-folding times after it saturates and enters the nonlinear stage considered here. (As discussed in Ref. 3, this single-wave model's solutions have direct relevance to models including the effects of sidebands.)

We describe the motion of the beam particles individually, while the behavior of the particles constituting the plasma is described by the linear plasma dielectric function  $\epsilon(\omega, k)$ . The beam particle motion is thus described by the usual force equation,

$$\dot{x}'_j = -(ike/m') \phi'(t) \exp[ikx'_j(t)] + c.c. \quad (1)$$

Here,  $\phi'(t)$  is the complex amplitude of the single mode,  $k$  is the wavenumber of the mode,  $x'_j(t)$  is the position of the  $j$ th beam particle in the laboratory frame, and  $e$  and  $m'$  are the charge and mass, respectively, of each beam particle. (The primes have been introduced to simplify the notation in the final equations, obtained in Part C of this section.)

Factoring out the dominant, unperturbed linear frequency  $\omega_0$  from  $\phi'(t)$  by writing  $\phi'(t) = \phi''(t) \exp -i\omega_0 t$  (or equivalently, making a Galilean transformation to the rest frame of the unperturbed wave), we turn Poisson's equation into a time-evolution equation for

the wave amplitude by casting it in the form

$$\begin{aligned} \exp(-i\omega_0 t) \epsilon(\omega_0 + i \partial/\partial t, k) \phi'' &= (4\pi e/k^2) n'(t) \\ &= (4\pi e/k^2) L^{-1} \sum_{j=1}^{N_0} \exp[-ikx'_j(t)]. \end{aligned} \quad (2)$$

Here  $n'(t)$  is the Fourier transform of the beam particle number density in the plasma rest frame,  $N_0$  is the number of beam particles in the system, and  $L$  is the length of the system. Assuming periodic boundary conditions, we take  $L = 2\pi/k =$  one wavelength. Using  $\omega_0 = kv_0$ , we transform this to the rest frame at  $t = 0$  of the beam and unperturbed wave:

$$\begin{aligned} \epsilon(\omega_0 + i\partial/\partial t, k) \phi'' &= (4\pi e/k^2) n''(t) \\ &= (4\pi e/k^2) L^{-1} \sum_{j=1}^{N_0} \exp[-ikx''_j(t)] \end{aligned} \quad (3)$$

where  $x''_j = x'_j - v_0 t$  and  $n''$  are the particle position and Fourier transformed density, respectively, in this frame. Finally, using the normal-mode condition  $\epsilon(\omega_0, k) = 0$  and expanding  $\epsilon$  to first order in  $\delta\omega \rightarrow (i\partial/\partial t)$ , we obtain the coupled set:

$$\phi'' = -(4\pi e i/k^2 \bar{\epsilon}) n'' = -(4\pi e i/k^2 \bar{\epsilon}) L^{-1} \sum_{j=1}^{N_0} \exp(-ikx''_j) \quad (4)$$

where  $\bar{\epsilon} = (\partial\epsilon/\partial\omega)_{k, \omega_0}$

$$\text{and} \quad \ddot{x}''_j = -(ike/m') \phi'' \exp(ikx''_j) + c.c. \quad (5)$$

(B) Initial Conditions-Linear and Post-Saturation Intervals

Equations (4)-(5) are the basic equations of motion used by O'Neil et al. for the self-consistent beam-plasma interaction. In addition, we must specify the initial conditions for the process being considered. These are (a) a uniform density beam with zero spread in particle velocity,  $v_j''(t=0) = v_j' - v_0 = 0$ ,  $x_j''$  evenly spaced over L, and (b) a very small wave amplitude, physically arising from thermal noise.

Thus in phase space  $(x'', v'')$ , the particle configuration at  $t = 0$  appears as a constant-density horizontal line at  $v'' = 0$ . This initial configuration will be periodic with period L for all t, but during the early, pre-saturation phase of the wave-development, it will be distorted in a complicated fashion. There are several effects contributing to the complexity. If the wave-trough shape were perfectly parabolic and time independent so that the particle bounce frequency were independent of how deeply it was trapped, the particle configuration in phase space would remain a straight line segment, rotating about the phase-point ( $x''$  is the trough center,  $v'' = 0$ ). For a sinusoidal trough, even if the amplitude and frequency of the wave were taken as fixed, the large dispersion in the bounce frequency of particles not too deeply trapped would cause a phase-mixing in this portion of the particle distribution. In addition, of course, the wave amplitude and frequency are changing, for early times, on a time-scale shorter than the particle bounce-time, introducing further phase-mixing effects, again especially strong on particles not well-trapped. As a result we expect the initially linear phase-space locus of particles to develop into

forms like those shown in Fig. 2(a), having a high density, roughly linear segment corresponding to well-trapped particles, with lower density (per unit length of this shape), highly phase-mixed filamentary tails streaming off the ends of the linear portion.

Owing to these considerations, we do not attempt to solve for the particle phase-space configuration at the beginning of the saturation stage of the interaction, but instead use the picture described here, supported by Fig. 2 (a), of the effect of the wave on the initial particle phase space configuration; that it will rotate one-wavelength segments of the particle configuration through some angle  $\alpha_0 = \alpha(t_0)$  at the onset  $t = t_0$  of the saturation stage, with the various dispersive effects operating to distort the bar from a strictly linear shape. At the extremities of the bar, strong dispersive effects will produce backward-bending, filamentary tails. In determining the time evolution of the wave, we shall have driving terms, in the equations of motion, like

687108400000



$\sum_j \exp i (kx_j'' - \theta)$ . Here,  $\theta$  is the wave phase angle. Due to the reduced density and large dispersion in phase of these tails at the bar ends, we expect these tails to produce negligible time-dependent effects. We shall therefore take our post-saturation interval initial conditions for the particle configuration to be a roughly linear, bar-like shape (the exact shape is not critical), and with length less than its  $t = 0$  one-wavelength value. The additional parameters describing the bar at  $t = t_0$  are  $\alpha_0$ , defined here,  $f \equiv$  the fraction of the  $N_0$  particles which we take to be in the non-dispersed bar-length, and  $\delta x_c$  is the displacement from the trough-bottom of the center of the bar. (We may choose to specify  $\delta x_c$ , as done here, setting the initial velocity  $\delta v_c$  of the bar center equal to zero, or specify  $\delta v_c$  and set  $\delta x_c = 0$ , or take any combination  $(\delta x_c, \delta v_c)$ . Specifying both, however, just introduces an additional phase angle into the problem, which we may set to any desired value by an appropriate translation in our origin of time.)

These we do not derive from first principles, but rather treat as fit parameters, evaluable from the results of O'Neil et al., presented in their Figs. 2 and 3, reproduced in our Figs. 1 and 2. The idealization of this configuration to strictly linear bars rotating in phase space, is illustrated in Fig. (2-b).

(C) Hamiltonian and Auxiliary Equations

We seek a Hamiltonian which gives the N-particle equations of motion, Eqs. (4) and (5). We find:

$$H = \sum_{j=1}^{N_0} H_j = \sum_{j=1}^{N_0} (K_j + V_j) \quad (6)$$

$$K_j = p_j''^2 / 2m \quad (7)$$

$$V_j = e \left[ \phi'' \exp(i k x_j'') + \phi''^* \exp(-i k x_j'') \right] \quad (8)$$

$$= 2e \phi_0'' \cos(k x_j'' - \theta)$$

where  $(x_j'', p_j'')$  are the canonically conjugate position and momentum of the  $j$ th particle, and  $\phi_0''$ ,  $\theta$  are defined by

$$\phi_0'' = |\phi''|, \quad \phi'' = \phi_0'' \exp -i\theta \quad (9)$$

In Eqs. (6-8), the wave variables are not in their canonical form. For these we may choose either the complex wave amplitude representation  $(\psi, p_\psi)$ , or we may transform these to action angle variables  $(\theta, J)$ . Here

$$\psi = (e/\beta) \phi'', \quad p_\psi = i\psi^* \quad (10)$$

and  $\beta$ (real) is determined from Hamilton's equations to satisfy

$$\beta^2 = e^2 (4\pi/\epsilon k^2 L) \quad (11)$$

$(\theta, J)$  are then defined as

$$J = |\psi|^2, \quad \psi = -J^{1/2} \exp -i\theta \quad (12)$$

In terms of the  $(\psi, p_\psi)$  representation, (8) becomes

$$V_j = \beta \psi \exp ikx_j'' - i\beta p_\psi \exp -ikx_j'' \quad (13)$$

In the  $(J, \theta)$  representation, Eq. (8) appears as

$$V_j = -2\beta J^{1/2} \cos(kx_j'' - \theta) \quad (14)$$

(We have chosen  $\theta$  in Eq. (12) to put the wave trough at  $kx_j'' - \theta = 0$ .)

Making the canonical transformation

$$x_j'', p_j'' \rightarrow x_j = kx_j'', \quad p_j = p_j''/k \quad (15)$$

we write  $H$  as

$$H = \sum_{j=1}^{N_0} H_j = K + V \quad (16)$$

$$H_j = K_j + V_j = (2m)^{-1} p_j^2 - 2\beta J^{1/2} \cos(x_j - \theta) \quad (17)$$

where

$$m \equiv m'/k^2$$

From Eqs. (16, 17) we have

$$\delta\omega_R(t) \equiv \dot{\theta}(t) = \partial H/\partial J = -\beta J^{-1/2} \sum_j \cos(x_j - \theta) \quad (18)$$

$$\begin{aligned} r(t) &\equiv \frac{1}{2} J/J = -(2J)^{-1} \partial H/\partial \theta \\ &= \beta J^{-1/2} \sum_j \sin(x_j - \theta) \end{aligned} \quad (19)$$

Combining these, we may write

$$\delta\omega(t) \equiv \delta\omega_R(t) + ir(t) = -\beta J^{-1/2} \sum_j \exp -i(x_j - \theta) \quad (20)$$

We have two conserved quantities,  $E = H$ , the total energy, and  $p$ , the total momentum (times the constant  $k^{-1}$ ). Using (18) we may write  $H$  in the form

$$H = \sum_j (2m)^{-1} p_j^2 + \int_0^J dJ' \delta\omega_R(J') \quad (21)$$

00004801790

Since  $\delta\omega_R(J) \sim J^{-1/2}$ , the second term in Eq. (21) is equal to  $2\delta\omega_R J$ , the form used in Ref. (1) to express H. This form is not in canonical form, however, and so might be misleading.

The second conserved quantity, the total momentum P, conserved because  $\theta$  and the  $x_j$  appear only in the combination  $(x_j - \theta)$  in H, is given by

$$P = \sum_j p_j + J \quad (22)$$

What is needed now is a means of reducing the number of degrees of freedom in the problem, while maintaining its essential physical aspects, including the two conservation laws just obtained. In the next section we describe how we go about this.

### III. THE REDUCED PROBLEM

In Part A of this section we introduce the central approximation of this paper, the "rotating bar model." As noted in the introduction, this approximation enables us to greatly reduce the number of degrees of freedom in our problem. Mathematically, the model amounts to applying a constraint on the particle positions, describing the positions of N particles in terms of the positions of only two. In Part B we discuss the general procedure for imposing this constraint on a Hamiltonian or Lagrangian formulation. The method may be useful in situations where a coherent or correlated behavior of a number of similar subsystems occurs (in the N-particle problem, the subsystems are the resonant particles). Part C applies the general method of Part B to the present problem.

#### (A) Rotating Bar Model

Now we wish to formalize the ideas involved in the rotating bar model. The basic idea, as mentioned in the introduction, is to describe the phase space trajectory  $\Gamma_j(t) = (x_j, p_j)$  of each particle as an average motion  $\Gamma_0(t)$  of the particles in a single wave trough, plus a revolving motion  $\delta\Gamma_j(t)$  about that center. The nature of the idealization is illustrated in Figure (2). In Figure (2-a), we draw from Fig. (3) of Ref. (1) the appearance of the locus in phase space of the trapped particles, at successive snapshots in time. In Fig. (2-b) we idealize the bar-like shapes in Fig. (2-a), keeping the approximate center position, orientation, and bar length, and truncating the filamentary tails. The phase space coordinates  $\Gamma_0(t)$ ,  $\Gamma_j(t)$ , and  $\delta\Gamma_j(t)$  are depicted in Fig. (3).

The equations of motion for the average phase space point  $\Gamma_0(t)$  are the same as those of a single particle located at  $\Gamma_0$ , namely

$$(d/dt)\Gamma_0 \equiv (d/dt)(x_0, p_0) = (\partial/\partial p_0)(p_0^2/2m), \quad -(\partial/\partial x_0)e\phi(x_0) \quad (23)$$

Expanding the Hamiltonian equations of motion for the  $j$ th particle at phase point  $\Gamma_j(t)$  about the nearby phase point  $\Gamma_0(t)$ , we deduce the equations of motion for  $\delta\Gamma_j(t) \equiv \Gamma_j(t) - \Gamma_0(t)$ :

$$(d/dt)\delta\Gamma_j \equiv (d/dt)[\delta x_j, \delta p_j] = \underline{H}(\Gamma_0) \cdot \delta\Gamma_j + \mathcal{O}(\delta\Gamma_j)^2 \quad (24)$$

where the rotation matrix  $R$  is given by

$$R(\Gamma_0) \equiv \begin{bmatrix} 0 & m^{-1} \\ \left. \frac{\partial^2 e}{\partial x^2} \right|_{x_0} & 0 \end{bmatrix} \quad (25)$$

Provided that

$$-R_{21} = \left. \frac{\partial^2 e}{\partial x^2} \right|_{x_0} > 0 \quad (\text{well-trapped particles}),$$

the matrix  $R$  has a form which generates an infinitesimal rotation in phase space. For given scales on the  $x$  and  $p$  axes, this rotation will, in general, involve a stretching or contraction of the linear-bar shape, just as would be the case for perfectly simple harmonic oscillation. The instantaneous frequency of revolution is given by

$$\omega_r^2(x_0) = -R_{21}R_{12} = -e\phi(x_0)/m. \quad (26)$$

[We recall in obtaining Eq. (26) that we have chosen  $x$  so that  $\phi(x) \sim \cos(x - \theta)$ , hence  $\partial^2 \phi / \partial x^2 = -\phi(x)$ .]

The term  $\mathcal{O}(\partial \Gamma_j)^2$  in (24) produces the anharmonic dispersive effects on the bar shape, discussed in Sec. II, B. Our approximation is to drop this dispersive term, for the portion of the bar not mixed away after the post-saturation interval has begun.

We now constrain the particle coordinates, writing  $x_j$  in terms of  $x_0$ , the position of a particle at the bar center, and  $x_s$ , the position of the particle at one end of the bar. We thus

take  $j$  to run from  $-s$  to  $s$  in running over the  $2s + 1 = N$  particles in the bar. Then we have

$$x_j = x_0 + (j/s)(x_s - x_0)$$

$$\dot{x}_j = \dot{x}_0 + (j/s)(\dot{x}_s - \dot{x}_0), \quad \text{and}$$

$$\dot{p}_j = m\dot{x}_j, \quad (j = -s, -s+1, \dots, s)$$

(27)

In writing (27) we have specified the phase-points  $\Gamma_j$  of the  $N \equiv fN_0$  particles in the bar (here  $f \equiv$  the fraction of beam particles which are in the bar) entirely in terms of the phase points  $\Gamma_0$  and  $\Gamma_s$  of particles at the bar center and bar end, respectively. If we impose this constraint upon the Hamiltonian  $H$  or Lagrangian  $L$  governing the system's time development, we obtain a new reduced Hamiltonian  $\tilde{H}$  or Lagrangian  $\tilde{L}$ , in terms of a reduced number of degrees of freedom (two degrees to describe the bar and one degree for the wave).

To complete the model, we must say something about the fraction  $(1-f)$  of particles in the filamentary tails. We assume that they are broadly spread in phase, so that their time-dependent effects vanish. We expect the tail particles to be approximately symmetrically distributed about the wave trough, so that the average of  $\sin(x_j - \theta)$ , over the tail, should vanish. Since the tail particles are shallowly trapped, we expect the tail-average  $\langle \cos(x_j - \theta) \rangle' \equiv C$  to be an approximately constant negative number,  $0 > C > -1$  (recalling that the wave crest is at  $(x_j - \theta) = \pm\pi$ ). Then, defining  $N_t = (1-f)N_0$ ,

the number of particles in the tail, we may write

$$\begin{aligned} \sum' \exp i(x_j - \theta) &= N_t (\exp i(x_j - \theta))' \\ &= N_t (\cos (x_j - \theta))' + i N_t (\sin (x_j - \theta))' \\ &\approx N_t C \end{aligned} \quad (28)$$

From Eqs. (18,19), we accordingly expect the tail contributions,

$\delta\omega_{R_t}$  and  $\delta\gamma_t$ , to  $\delta\omega_R$  and  $\gamma$ , to be

$$\delta\omega_{R_t} = -\beta J^{-\frac{1}{2}} N_t C \quad (29)$$

$$\delta\gamma_t = 0 \quad (30)$$

From (14), we expect a contribution  $V_t$  to  $V$ ,

$$V_t = -2\beta\sqrt{J} N_t C \quad (31)$$

The kinetic energy contribution of the tail, which we also take to be time independent, just gives an additive constant to  $H$ , which we drop.

### (B) General Reduction Procedure

Equations (27), which are the mathematical statement of the rotating-bar model, amount to a set of  $(N-2)$  holonomic constraints on the coordinates  $x_j$ , expressing all the  $x_j$  in terms of only

$x_0$  and the relative coordinate  $\xi \equiv x_s - x_0$ . Such a constraint is easily applied to a Lagrangian formulation of the problem. However, we are working with a Hamiltonian formulation. We thus seek in this subsection to find a prescription for applying the constraint equations (27) to a Hamiltonian. We begin by constraining the Lagrangian of the problem, which we write in the general form

$$L = L(x_j, \dot{x}_j, Q) = L_0(Q) + \sum_{j=1}^N L_1(x_j, \dot{x}_j; Q) \quad (32)$$

The parameter  $Q$  here represents the set of wave variables, which do not enter into the reduction procedure, and so we drop  $Q$  from explicit notation.  $L_1$  is the contribution of a single particle to the Lagrangian. Let us denote the set  $(x_0, \xi)$  of the reduced variables by the more general notation  $(q_k)$ . Then we write the constraint equations (27) more generally as

$$\begin{aligned} x_j &= x[(q_k), j/s] \\ \dot{x}_j &= v[(q_k, \dot{q}_k), j/s], \quad p_j = m\dot{x}_j \end{aligned} \quad (33)$$

If we now write the Lagrangian (32), replacing  $x_j$  and  $\dot{x}_j$  there by their constrained description in terms of the reduced set of coordinates  $(q_k, \dot{q}_k)$ , Eqs. (33), we obtain the reduced Lagrangian  $\tilde{L}$ :

$$\tilde{L}(q_k, \dot{q}_k) \equiv L_0 + \sum_{j=1}^N L_1[x((q_k), j/s), v((q_k, \dot{q}_k), j/s)] \quad (34)$$

The equations of motion for the reduced coordinates then come from the usual Lagrangian prescription, i.e.,

$$0 = (d/dt) \partial \tilde{L} / \partial \dot{q}_k - \partial \tilde{L} / \partial q_k. \quad (35)$$

In writing (27) we are assuming that the  $q_k(t)$  evolve in time such as to make  $\int dt \tilde{L}(t)$  an extremum, just as the  $x_j(t)$  evolve in time so that  $\int dt L(t)$  is an extremum. The set of possible motions of the  $x_j(t)$  described by the constraint equations (33) are a proper subset of the unconstrained problem. Thus to the extent that our constraint equations (33) are valid, the reduced variables  $q_k(t)$  should develop in time in such a manner as to accurately describe the time evolution of the full problem.

We may generalize Eq. (34) slightly, allowing the discrete distribution of particles along the bar to become a continuous one, with the discrete parameter  $j/s$  replaced by a continuous parameter  $\lambda$ , the  $\sum_j$  in (34) to become an  $\int d\lambda$ . We thus write

$$\tilde{L}(q_k, \dot{q}_k) = L_0 + \int d\lambda F(\lambda) L_1 [x((q_k), \lambda), v((q_k, \dot{q}_k), \lambda)] \quad (36)$$

Here  $F(\lambda)$  is the density distribution of the particles along the bar, normalized to  $N$ . If we wish to recover the discrete notation in (34), we may simply take

$$F(\lambda) = \sum_{j=1}^N \delta[\lambda - (j/s)] \quad (37)$$

We may use either the discrete or continuous forms for  $L_{red}$ . We choose to use the continuous form, Eq. (36).

For the Hamiltonian formulation we proceed similarly, except that we must be careful in obtaining the momenta  $P_k$  canonically conjugate to the  $q_k$ . We do this via the Lagrangian definition:

$$\begin{aligned} P_k &\equiv \partial \tilde{L} / \partial \dot{q}_k = (\partial / \partial \dot{q}_k) \int d\lambda F(\lambda) L_1 [x((q_\ell), \lambda), v((q_\ell, \dot{q}_\ell), \lambda)] \\ &= \int d\lambda F(\lambda) (\partial L / \partial v) (\partial v / \partial \dot{q}_k) \end{aligned} \quad (38)$$

Using  $p = \partial L / \partial v$ , we write (38) as

$$P_k = \int d\lambda F(\lambda) p \partial v / \partial \dot{q}_k \quad (39)$$

This expresses  $P_k$  wholly in terms of things known from a Hamiltonian formulation of the full problem. We may thus apply the reduction procedure analogous to Eq. (36) to the full Hamiltonian  $H$ , and reexpress this  $\tilde{H}$  in terms of the canonical variables  $(q_k, P_k)$ . The equations of motion, equivalent to (35), are then the usual Hamiltonian equations coming from  $\tilde{H}$ .

### (C) Reduced Hamiltonian

We now apply the general procedure just described to the specific problem at hand. The constraint equations (33) are given by the rotating bar model (27), and we take a constant density bar, with  $\lambda$  running from minus one to one:

$$F(\lambda) = N/2 = \text{constant} \quad (40)$$

We write (16,17) in the form of (32) as

$$H = H_0 + \sum_{j=1}^N H_1 \quad (41)$$

$$H_0 = V_t(J) = -2\beta N_t C \sqrt{J} \quad (42)$$

$$H_1(x_j, p_j; \theta, J) = (p_j^2/2m) - 2\beta \sqrt{J} \cos(x_j - \theta) \quad (43)$$

From (27) we have the new dynamical variables

$$q_1 \equiv x_0, \quad q_2 \equiv \xi \equiv x_s - x_0 \quad (44)$$

Following the prescription (34), we write

$$\begin{aligned} \tilde{H} &= H_0 + \int_{-1}^1 d\lambda f(\lambda) H_1[x(x_0, \xi; \lambda), p(x_0, \xi; \lambda)] \\ &= H_0 + (N/2) \int_{-1}^1 d\lambda [p^2/2m - 2\beta \sqrt{J} \cos(x - \theta)] \quad (45) \end{aligned}$$

The canonical momenta  $P_0, P_\xi$  are obtained using prescription (39):

$$\begin{aligned} P_0 &= \int_{-1}^1 d\lambda F(\lambda) p(\dots; \lambda) \partial v / \partial \dot{x}_0 \\ &= (N/2) \int_{-1}^1 d\lambda m(\dot{x}_0 + \lambda \dot{\xi}) = Nm \dot{x}_0 \quad (46) \end{aligned}$$

and similarly

$$P_\xi = (N/2) \int_{-1}^1 d\lambda m(\dot{x}_0 + \lambda \dot{\xi}) \lambda = (N/3) m \dot{\xi} \quad (47)$$

Carrying out the integration in (45) and using (46-47), we finally get

$$\begin{aligned} \tilde{H}(x_0, P_0; \xi, P_\xi; \theta, J) &= \tilde{K} + \tilde{V} + V_t \\ &= (P_0^2 + 3P_\xi^2)(2mN)^{-1} - 2\beta J^{1/2} [ND(\xi) \cos(x_0 - \theta) + N_t C], \quad (48) \end{aligned}$$

where

$$D(\xi) \equiv \sin \xi / \xi \quad (49)$$

The factor  $D$  comes from performing the integration  $\int_{-1}^1 d\lambda \cos[x_0 - \theta + \lambda \xi]$  prescribed by Eq. 45. Analogous to (18)-(20) this reduced form gives

$$\begin{aligned} \delta \omega_R(t) \equiv \dot{\theta}(t) &= \partial \tilde{H} / \partial J \\ &= -\beta J^{-1/2} [ND(\xi) \cos(x_0 - \theta) + N_t C] \quad (50) \end{aligned}$$

$$r(t) \equiv J(t)/2J = \beta J^{-1/2} ND(\xi) \sin(x_0 - \theta); \quad (51)$$

and combining these,

$$\delta \omega(t) \equiv \delta \omega_R + i\gamma = -\beta J^{-1/2} [ND(\xi) \exp -i(x_0 - \theta) + N_t C] \quad (52)$$

Analogous to (21, 22), we again have conservation of energy

$\tilde{H}$  and momentum  $P$ :

$$\tilde{H} = \tilde{K} + 2\delta \omega_R J \quad (53)$$

$$P = P' - P_t = P_0 + J = Nm\dot{x}_0 + J. \quad (54)$$

Here  $P'$  is the total momentum of the  $N$  particle system, and  $P_t$  is the momentum of the particles in the tail.

Energy conservation was maintained in carrying out the reduction procedure simply by keeping to a Hamiltonian formalism, i.e., by obtaining  $\tilde{H}$  from  $H$ . Momentum conservation holds in the reduced problem for essentially the same reason as it held in the full problem, namely that the system is invariant under a displacement of the entire wave-plus-particles system. We also note that the momentum depends only on the  $P_0$  momentum and not on the variables  $\xi, P_\xi$ . Physically, this is to be expected, since the momentum of the  $j$ th and  $(-j)$ th particles in the bar is  $p_0 + m(j/s)(\dot{x}_s - \dot{x}_0) + p_0 - m(j/s)(\dot{x}_s - \dot{x}_0) = 2p_0$ , i.e., the relative momenta cancel.

We now use  $P$ -conservation to further simplify the problem from three to two degrees of freedom. We choose to eliminate the wave variables. Introducing the generating function

$$S(x_0, \xi, \theta; \tilde{P}_\eta, \tilde{P}_\xi, \tilde{P}) = \tilde{P}_\eta(x_0 - \theta) + \tilde{P}\theta + \tilde{P}_\xi\xi, \quad (55)$$

we transform from  $(x_0, \xi, \theta; P_0, P_\xi, J)$  to  $(\eta, \tilde{\xi}, \tilde{\theta}; \tilde{P}_\eta, \tilde{P}_\xi, \tilde{P})$  by the usual prescription.<sup>10</sup> We have used only the identity transformation for the variables  $\tilde{\xi}, P_\xi$ , i.e., we have  $\tilde{\xi} = \xi, \tilde{P}_\xi = P_\xi$ , and so we drop the tildes on these symbols, as well as on  $\tilde{P}_\eta$ , for simplicity of notation. For the other variables we have

$$P_\eta = P_0, \quad \eta = x_0 - \theta, \quad \tilde{\theta} = \theta, \quad \tilde{P} = P_0 + J. \quad (56)$$

From (54) we see that the new momentum  $\tilde{P}$  here has the same significance as  $P$  had there, the total momentum of the system, a constant. Hence  $\tilde{\theta} = \theta$  is an ignorable coordinate. The new coordinate  $\eta$  is the position of the bar center relative to the trough bottom. Since  $\tilde{P} = P$  and  $\tilde{\theta} = \theta$ , we retain the old symbols  $P, \theta$  in our transformed  $\tilde{H}$ .

$$\begin{aligned} \tilde{H}(\eta, P_\eta; \xi, P_\xi; P) &= (P_\eta^2 + 3P_\xi^2)(2mN)^{-1} \\ &\quad - 2\beta(P - P_\eta)^{\frac{1}{2}}[ND(\xi) \cos \eta + N_t C] \end{aligned} \quad (57)$$

We now seek means of solving the corresponding equations of motion, coming from this  $\tilde{H}$ .

#### IV. SOLUTION OF THE REDUCED PROBLEM

We have now reduced the full  $N$ -particle problem to one involving only two degrees of freedom. The equations of motion are nonlinear. To proceed further, we may either introduce some additional approximations, allowing further analytic progress, or numerically integrate the equations of motion, for specified initial conditions. We shall follow both of these alternatives.

We first follow the former route, namely linearizing the full equations of motion coming from (57) about a fixed point which is appropriate to the physical situation under consideration.

The equations of motion are

$$\dot{\eta} = \frac{\partial \tilde{H}}{\partial P_\eta} = (mN)^{-1}P_\eta + \beta J^{-\frac{1}{2}}[ND(\xi) \cos \eta + N_t C] \quad (58)$$

00004801792



$$\dot{\xi} = (3/mN)P_{\xi} \quad (59)$$

$$\dot{P}_{\eta} = -2\beta J^{\frac{1}{2}}ND(\xi) \sin \eta \quad (60)$$

$$\dot{P}_{\xi} = 2\beta J^{\frac{1}{2}}ND'(\xi) \cos \eta \quad (61)$$

where

$$D'(\xi) \equiv dD/d\xi;$$

we recall that the wave action  $J = P - P_{\eta}$  is to be described in terms of the new variables  $P, P_{\eta}$ .

The fixed points are determined by setting the left sides of Eqs. (58-61) equal to zero. Doing this, one obtains several possible fixed point solutions, but only one of them corresponds to the case of interest. We shall denote by  $h^0$  the fixed point value of any dynamical variable  $h$ . The relevant fixed point satisfies the following:

a) The bar center lies at the wave trough, rather than at the crest, for which the equilibrium would be unstable. Thus

$$\eta^0 = 0 \quad (62)$$

(instead of  $\eta^0 = \pm \pi$ ).

b) The unperturbed (i.e., fixed) bar has zero length in phase space,

$$\xi^0 = P_{\xi}^0 = 0, \quad (63)$$

so that the resonant particles in this fixed point, steady state condition form a single "superparticle".

c) There is a finite-amplitude wave, i.e.,

$$J_0 > 0. \quad (64)$$

Equation (60) is satisfied identically because of (62), as is (61) because of (63). Finally, Eq. (58) is a statement that the steady state particle velocity (negative in the initial beam rest frame) is equal to the steady-state wave phase velocity, so that the particles maintain a steady-state phase relation with the wave. It yields a condition determining the steady-state wave action  $J_0$ , or equivalently particle momentum  $P_{\eta}^0$ :

$$-P_{\eta}^0 [P - P_{\eta}^0]^{\frac{1}{2}} = \beta mN[N + N_t C]. \quad (65)$$

Since the saturation wave amplitude is roughly equal to this steady state value, Equation (65) gives an approximate expression for the wave saturation amplitude. (However, it is still a function of the as yet undetermined constants  $P, f \equiv N/N_0$ , and  $C$ .)

Equations (62-65) determine the fixed point values  $\eta^0, P_{\eta}^0, \xi^0, P_{\xi}^0$ . We now linearize Eqs. (58-61) about this fixed point, writing  $h' \equiv h - h^0$  for all variables  $h$ . Physically this corresponds to perturbing the particles from the steady-state situation, allowing the particles as a whole to slosh back and forth in the wave trough ( $\eta', P_{\eta}' \neq 0$ ), and introducing a finite spatial and momentum spread ( $\xi', P_{\xi}' \neq 0$ ). The linearized

equations of motion are

$$\begin{aligned} \dot{\eta}' &= \left[ (mN)^{-1} + \frac{1}{2} \beta J_0^{-3/2} (N + N_{tC}) \right] P_{\eta}' \\ &= (mN)^{-1} \left( 1 - \frac{1}{2} P_{\eta}^0 / J_0 \right) P_{\eta}' \end{aligned} \quad (66)$$

$$\dot{P}_{\eta}' = -2\beta N J_0^{\frac{1}{2}} \eta' \quad (67)$$

$$\dot{\xi}' = (3/mN) P_{\xi}' \quad (68)$$

$$\dot{P}_{\xi}' = -(2\beta/3) N J_0^{\frac{1}{2}} \xi' \quad (69)$$

Thus, to first order about the fixed point, we see that the motion decouples into two simple harmonic oscillator systems  $(\eta', P_{\eta}')$  and  $(\xi', P_{\xi}')$ , having frequencies  $\omega_{b0}$  and  $\omega_{r0}$ , respectively, given by

$$\omega_{b0}^2 = 2\beta m^{-1} J_0^{\frac{1}{2}} \left( 1 - \frac{1}{2} P_{\eta}^0 / J_0 \right) \quad (70)$$

$$\omega_{r0}^2 = 2\beta m^{-1} J_0^{\frac{1}{2}} \quad (71)$$

Comparing (71) and (26), we find that  $\omega_{r0}^2 = \omega_r^2(x_0 = 0)$ , i.e., the reduced Hamiltonian formalism and the simpler analysis of Section (III-A) give the same result for the bar revolution frequency.

Comparing (70) and (71), we see  $\omega_{b0}^2$  is enhanced over  $\omega_{r0}^2$  by the factor  $(1 - \frac{1}{2} P_{\eta}^0 / J_0) > 1$ . The second term  $\Delta_0 \equiv -\frac{1}{2} P_{\eta}^0 / J_0$  in ( ) here comes from the second term in ( ) in (66), which corresponds to the contribution to  $\dot{\eta}$  from  $\dot{\theta}$ , i.e., the self-consistent wave response to the particle sloshing. As the particles slosh in one direction in the wave trough, the wave responds in the opposite direction. The particles thus see an effectively steeper potential well, and so bounce more rapidly. The revolution frequency  $\omega_r$ , however, depends only on the wave curvature at the bar center. Since this curvature varies only to the second order in the displacement  $\eta$  of the bar center from the wave trough,  $\omega_r$  is unaffected, to the first order, by the wave response.

For larger perturbations away from the fixed point, we would find those effects one expects from any coupled, anharmonic oscillation problem. These include: (i) an amplitude dependent shift in the bounce and revolution frequencies, due to the anharmonic shape of the wells in which the coordinates  $\eta$  and  $\xi$  are oscillating; (ii) a shift (again amplitude dependent) in the time-averaged drift velocity  $\langle \theta \rangle_t = \langle \partial \omega_R \rangle_t$  of the wave-particle system. (This velocity is negative in the rest frame of the unperturbed (i.e., beamless) wave, by momentum conservation.) Also we expect (iii) some coupling of the two oscillators.

The exact value of the factor  $\Delta_0$  is dependent, through Eq. (65), on the as yet free parameters  $f$  and  $P$ . In Eqs. (72-74) below, we shall relate these two parameters, still leaving  $f$  as a parameter undetermined by our model. Thus the value of  $\omega_b^2 / \omega_r^2 = 1 + \Delta$  for nonlinear oscillations is  $f$  dependent as well as amplitude dependent. For this reason we do not precisely

00004801793

calculate  $\Delta$  (the nonlinear generalization of  $\Delta_0$ ) from our model, but shall rather infer the value of  $\Delta$  from the results of

Réf:-1. From there, we expect to have  $|\Delta| \ll 1$ , i.e.,  $\omega_b \approx \omega_r$ .

For the linear case, we can estimate  $\Delta$  in terms of  $f$ , by assuming that the average momentum  $p_t^n$  of a particle in the tail is the same as the fixed-point value of the bar particles,  $p_t^n = P_\eta^0/N$ . The total momentum  $P'$  of the (wave + bar + tail) system, exactly conserved by Eq. (22), is equal to zero, because at  $t = 0$  there were negligible wave action and an unperturbed beam, which had zero velocity in the unperturbed wave-beam rest frame. We then have

$$\begin{aligned} 0 = P' &= J_0 + P_\eta^0 + P_t = J_0 + (1 + N_t/N)P_\eta^0 \\ &= J_0 + f^{-1}P_\eta^0 \end{aligned} \quad (72)$$

where we define  $P_t \equiv N_t p_t^n$ . Thus

$$J_0 = -f^{-1}P_\eta^0 \quad (73)$$

$$\Delta_0 = -\frac{1}{2} P_\eta^0 / J_0 = f/2 \quad (74)$$

For example, if we take  $f = \frac{1}{2}$ , then

$$\omega_{b0}/\omega_{r0} \approx 1.12 \quad (75)$$

For excursions from the fixed-point values of nonlinear amplitude in the  $\eta$  and  $\xi$  systems, we still expect the systems to oscillate about their time-averaged values. The time dependence of the oscillations will no longer be strictly sinusoidal, due to the anharmonic nature of the restoring forces the two systems see. However, we shall see that the highly nonlinear characteristics of the functions  $\delta\omega_R(t)$  and  $\gamma(t)$  come principally not from the anharmonic nature of these oscillations, but rather from the fact that  $\delta\omega_R$  and  $\gamma$  are highly nonlinear functions of these oscillatory solutions. To see this, we approximate the solutions for the dynamical variables by exactly sinusoidal functions of time:

$$\eta'(t) = \bar{\eta} \sin(\omega_b t + \phi_\eta) \quad (76)$$

$$P'_\eta(t) = \bar{P}_\eta \cos(\omega_b t + \phi_\eta) \quad (77)$$

$$\xi'(t) = \bar{\xi} \sin(\omega_r t + \phi_\xi) \quad (78)$$

$$P'_\xi(t) = \bar{P}_\xi \cos(\omega_r t + \phi_\xi) \quad (79)$$

where from (66,67),

$$\bar{P}'_\eta = mN(1 + \Delta)^{-1} \omega_b \bar{\eta}, \quad \bar{P}'_\xi = (mN/3) \omega_r \bar{\xi} \quad (80)$$

and

$$\omega_b = (1 + \Delta)^{\frac{1}{2}} \omega_r \approx (1 + \Delta/2) \omega_r \quad (81)$$

This approximation is supported by the good agreement between the analytic expressions we obtain for  $\delta\omega_R(t)$  and  $r(t)$  when we substitute (76-81) into (50,51), and the results we obtain from numerically integrating the full nonlinear equations of motion (58-61). The point to notice is the one noted just above, that the nonlinear characteristics of  $\delta\omega_R(t)$  and  $r(t)$  come mainly from their highly nonlinear dependence [cf. Eqs. (50-51)] on the oscillatory functions of time  $\eta$ ,  $P_\eta$ ,  $\xi$ , and  $P_\xi$ .

To complete the preparation for obtaining results, two details remain. First, we convert all quantities to dimensionless variables. We scale time by the linear (simple harmonic) revolution frequency  $\omega_{r0}$ , and the momenta to units of the steady state wave action  $J^0$ . This is done most conveniently by rescaling the Hamiltonian. Defining  $\mathcal{H} \equiv h \tilde{H}$ , we choose  $h$  by requiring that our new dimensionless variables, with  $(\partial/\partial t)$  replaced by  $(\partial/\partial \tau) \equiv \omega_{r0}^{-1}(\partial/\partial t)$ , obey Hamilton's equations. We then have:

$$\tau = \omega_{r0} t$$

$$\pi_\eta = P_\eta/J^0, \quad \pi_\xi = P_\xi/J^0, \quad \Pi = P/J^0, \quad \mathcal{J} = J/J^0 \\ = \Pi - \pi_\eta$$

$$\mathcal{H} = (2\mu f)^{-1}(\pi_\eta^2 + 3\pi_\xi^2) - \mu \mathcal{J}^{\frac{1}{2}} [fD(\xi) \cos \eta + f_t C]$$

where

$$\mu \equiv MN_0 \omega_{r0} / J_0$$

This is the scaled form of Eq. (57). From this we obtain the scaled forms of Eqs. (50-52):

$$\Omega_R \equiv \delta\omega_R/\omega_{r0} \equiv \partial \mathcal{H} / \partial \mathcal{J} = -\mu \mathcal{J}^{-\frac{1}{2}} [fD(\xi) \cos \eta + f_t C] \quad (83)$$

$$\Omega_I \equiv r/\omega_{r0} = \mu \mathcal{J}^{\frac{1}{2}} fD(\xi) \sin \eta \quad (84)$$

$$\Omega \equiv \Omega_R + i\Omega_I = -\mu \mathcal{J}^{-\frac{1}{2}} [fD(\xi) \exp -i\eta + f_t C] \quad (85)$$

Finally, we still have a number of parameters to evaluate which are left free in our model. These have to do with the initial conditions for the post-saturation interval of the beam-plasma interaction. In (76-79), we need the amplitudes  $\bar{\eta}$  and  $\bar{\xi}$ , and the relative initial phase  $\phi_0 \equiv (\phi_\xi - \phi_\eta)$  of the two oscillating systems. Then, if we use the model (72-74), we need only further specify  $f$ , the fraction of particles in the rotating bar, and  $C$ , a measure of where in the wave the particles in the tail spend most of their time. We thus have 5 parameters to specify. We do this by comparison with the information given in Figures 2 and 3 of Ref. (1). The phase  $\phi_0$  can be roughly obtained from Figure 3 there. The other parameters may be approximately evaluated by fitting characteristics of the results of Ref. 1 (their Fig. 2; our Fig. 1) to results obtained from the rotating bar model. The amount of arbitrariness in this fitting procedure is not nearly as large as the number of free parameters might lead one to suspect, however. Varying the parameters leads to some quantitative

000004801794

variation of results, but the qualitative features of the curves for  $\delta\omega_R(t)$  and  $r(t)$  obtained by O'Neil et al., enumerated in the introduction, are all reproduced by the rotating bar results, for wide ranges of values of these free parameters.

## V. RESULTS AND DISCUSSION

In Fig. 4 we reproduce the N-particle results of O'Neil et al., shown in full in Fig. 1, for the post-saturation portion of the interaction. The coordinate axes have been rescaled to conform approximately to our dimensionless variables. We have assumed that the ratio  $\omega_b/\omega_{r0}$  in the N-particle results is the same as in our numerical integration, i. e., we have synchronized the bounce periods. Doing this determines the rescaling of the frequency axis from Ref. 1 to here.

In Figures 5 and 6 we show the results of numerical integration of the exact equations of motion for the reduced problem, for the particular choice of parameters indicated in the figure captions.

Comparing Figure 4 with Figures 5 and 6, we see that the N-particle results are in strong qualitative agreement with those of our numerical integration, but that the N-particle amplitudes are somewhat larger than ours, for the particular choices of free parameters which we have made. The exact quantitative agreement is not particularly important, however, in view of these free parameters in the reduced problem.

In Fig. 5, we have set  $\xi = 0$ , i. e., we have set the bar length equal to zero, and so have only a single "superparticle," composed of the N bar particles at the same phase-point, sloshing in the wave trough. The  $\eta$ -degree of freedom is thus the only degree of freedom left in the problem, and so the nonlinear problem

can be solved exactly in terms of quadratures. We see that the superparticle solution has most of the features of the N-particle results; the sawtoothed form of  $\gamma$ , the phase relation between  $\delta\omega_R(\Omega_R)$  and  $\gamma(\Omega_I)$ , and the components at  $\omega_b$  and  $2\omega_b$  in  $\delta\omega_R$ . However the component at  $2\omega_b$ , creating the shallower troughs in  $\delta\omega_R$ , is not as pronounced in Fig. 5(a) as in the N-particle results, Fig. 4(a). When we allow the bar to have a finite length,  $\xi = 1.0$  [Figs. 6(a,b)], we see that the  $2\omega_b$ -component in  $\Omega_R$  becomes more pronounced, the other features of the  $\Omega_R$ ,  $\Omega_I$  curves remaining about the same. That the effect of the finite bar length should be to contribute to  $\Omega_R(\tau)$  a component at  $2\omega_r \approx 2\omega_b$  is to be expected; the bar rotating through  $\pi$  radius in phase space brings it back to physically the same position. The frozen-wave models, using energy-conservation arguments, also arrived at this expectation. However these analyses do not account properly for the other (superparticle) contributions to  $\Omega_R$ .

In Figures (7,8) we plot the explicit expressions which the linear reduced-problem gives for  $\Omega_R$  and  $\Omega_I$ . The same parameter values as used in Figs. (5) and (6) are used here, with one distinction. In Figures 5 and 6, the frequencies  $\omega_b$  and  $\omega_r$  which give rise to the particular time dependence of  $\Omega_R$  and  $\Omega_I$  are the nonlinear values, reducing to their linear (simple harmonic) values  $\omega_{b0}$ ,  $\omega_{r0}$  in the limit of small perturbation from the fixed point. They arise naturally in the time scale of  $\Omega_R(\tau)$ ,  $\Omega_I(\tau)$  from direct numerical integration of the equations of motion. In contrast, in Figs. 7 and 8 we have simply plugged the linear values  $\omega_{b0}$ ,  $\omega_{r0}$  into the explicit expressions for  $\Omega_R(\tau)$ ,  $\Omega_I(\tau)$

obtained by using the sinusoidal solutions, Eqs. (76-79), in Eqs. (83,84). Figures 7 and 8 are thus simply plots of two explicit functions of  $\tau$ , parametrically dependent on the values of  $\omega_D, \omega_r$  we choose to use there. Aside from this slightly different scaling of the time axes, we note the good agreement between the two reduced problem solutions, Figs. (5,6) and Figs. (7,8), and between these reduced problem results and the full N-particle problem results obtained in Ref. 1, Fig. 4.

#### VI. SUMMARIZING DISCUSSION

With regard to the specific problem studied in this paper, namely that of Ref. 1, we have found a model which is simple enough to obtain explicit expressions for the results, and yet which contains enough of the essential physics of the full problem that the explicit results which it yields are in very good qualitative agreement with the exact numerical results of O'Neil et al. The model allows for the self-consistent interaction of the wave and particles, which leads to results not expected from the frozen-wave approaches used previously.

In the process of formalizing the rotating bar concept, we have introduced a general technique for reducing the number of degrees of freedom in a problem, whenever the phase space trajectories of the separate degrees of freedom can be approximately described in terms of fewer free variables than the full  $2N$  coordinates and momenta present in  $N$  degrees of freedom. For coherent motions, such as is present in trapped-particle phenomena, such a description becomes possible.

If we wish to apply the technique to other problems involving resonant-particle-wave interactions, extensions of the method may become necessary. For example, the bar shape desired may be curved rather than linear in phase space, or the resonant particles may come from the plasma distribution itself, and so fill out a two-dimensional locus in phase space. In both cases, the new feature appearing is that we can no longer write our constraint equations in the simple form of Eqs. (27) or (33), in which the coordinates  $x_j$  are expressible just in terms of the reduced coordinates  $q_k$  (and the parameter  $\lambda_j = j/s$ ). We may instead generalize the form of the constraint equations, making the replacements, in going from  $L(x_j, \dot{x}_j)$  to  $\tilde{L}\{q_k, \dot{q}_k\}$ ,

$$x_j \rightarrow x[(q_k, \dot{q}_k), \lambda_j]$$

$$\dot{x}_j \rightarrow v[(q_k, \dot{q}_k), \lambda_j] .$$

(86)

This more general set of constraints is no longer of the type conventionally encountered in Lagrangian mechanics. Thus, although the reduction procedure described in Sec. III, Part B may be formally carried through, until a concrete application of this more general formalism is made, judgement on its mathematical validity and usefulness must be postponed.

Another possible direction of extension of this technique is to problems involving the interaction of resonant particles with several waves. For example, coherent trapped particle motions are present even in a turbulent plasma, as first discussed

567108004801795

by Dupree.<sup>11</sup> The methods used here could possibly be adapted to deal with such situations, by explicitly incorporating the phase-mixing effects into the model, giving the coherent phase-space rotations a finite lifetime.

#### ACKNOWLEDGMENT

This work was supported by the U. S. Energy Research and Development Administration, Division of Magnetic Fusion Energy.

#### REFERENCES

1. T. M. O'Neil, J. H. Winfrey, and J. H. Malmberg, *Phys. Fluids* 14, 1204 (1971).
2. M. Lampe and P. Sprangle, *Phys. Fluids* 18, 475 (1975).
3. T. M. O'Neil and J. H. Winfrey, *Phys. Fluids* 15, 1514 (1972).
4. G. J. Morales and T. M. O'Neil, *Phys. Rev. Lett.* 28, 417 (1972).
5. T. M. O'Neil, *Phys. Fluids* 8, 2255 (1965).
6. B. L. Cohen and A. N. Kaufman, *Phys. Fluids* 20, 1113 (1977).
7. J. M. Canosa, *Phys. Fluids* 19, 1952 (1976).
8. P. J. Vidmar, J. H. Malmberg, and T. P. Starke, *Phys. Fluids* 19, 32 (1976).
9. J. Canosa and J. Gazdag, *Phys. Fluids* 17, 2030 (1974).
10. H. Goldstein, *Classical Mechanics* (Addison-Wesley, Reading Massachusetts, 1965), p. 237ff.
11. T. H. Dupree, *Phys. Fluids* 15, 334 (1972). For similar ideas, see also, B. B. Kadomtsev and O. P. Pogutse, *Phys. Rev. Lett.* 25, 1155 (1970).

FIGURE CAPTIONS

Fig. 1. Reproduction of the simulation results obtained in Ref. 1, for the nonlinear frequency shift  $\Omega_R$  and growth rate  $\Omega_I$  as functions of time. Time  $t_0$  marks the beginning of the post-saturation interval of the wave-beam interaction, which is the time interval considered in this paper.

Fig. 2. (a) Reproduction from Ref. 1 of the locus in phase space of the trapped particles at successive snapshots in time. (b) The rotating bar idealization of Figure (2-a), used as the central approximation of this paper.

Fig. 3. Depiction of the rotating bar in phase space at an arbitrary time  $t$ . The phase space coordinates describing the bar and the particles which constitute it are displayed, for the particular choice of  $N \equiv$  number of particles in the bar  $= 2s + 1 = 9$ . These coordinates are:  $\Gamma_0 \equiv (x_0, p_0) =$  bar center position;  $\Gamma_j \equiv (x_j, p_j) =$  phase position of the  $j$ th particle, here shown for  $j = s = 4$ ;  $\delta\Gamma_s \equiv (x_s - x_0, p_s - p_0) =$  position of the  $s$ th particle (the particle at the bar's end) relative to the bar center.

Fig. 4. Post-saturation interval of the simulation results of Ref. 1 shown in full in Fig. 1. The coordinate axes have been rescaled to conform to the dimensionless variables used in this paper.

Fig. 5. Results of numerical integration of the exact (nonlinear) equations of motion for the reduced (rotating bar) problem. The choices of free parameters used for the integration are:  $f = 0.4$ ,  $C = -0.1$ ,  $\phi_0 = -\pi(\omega_r/\omega_b) \approx -2.868$ ,  $\bar{\pi}_\eta \equiv \bar{P}_\eta/J^0 = 0.65$ ,  $\bar{\xi} = 0$ .

Fig. 6. Same as Fig. 5, but for a nonzero bar length,  $\bar{\xi} = 1$ .

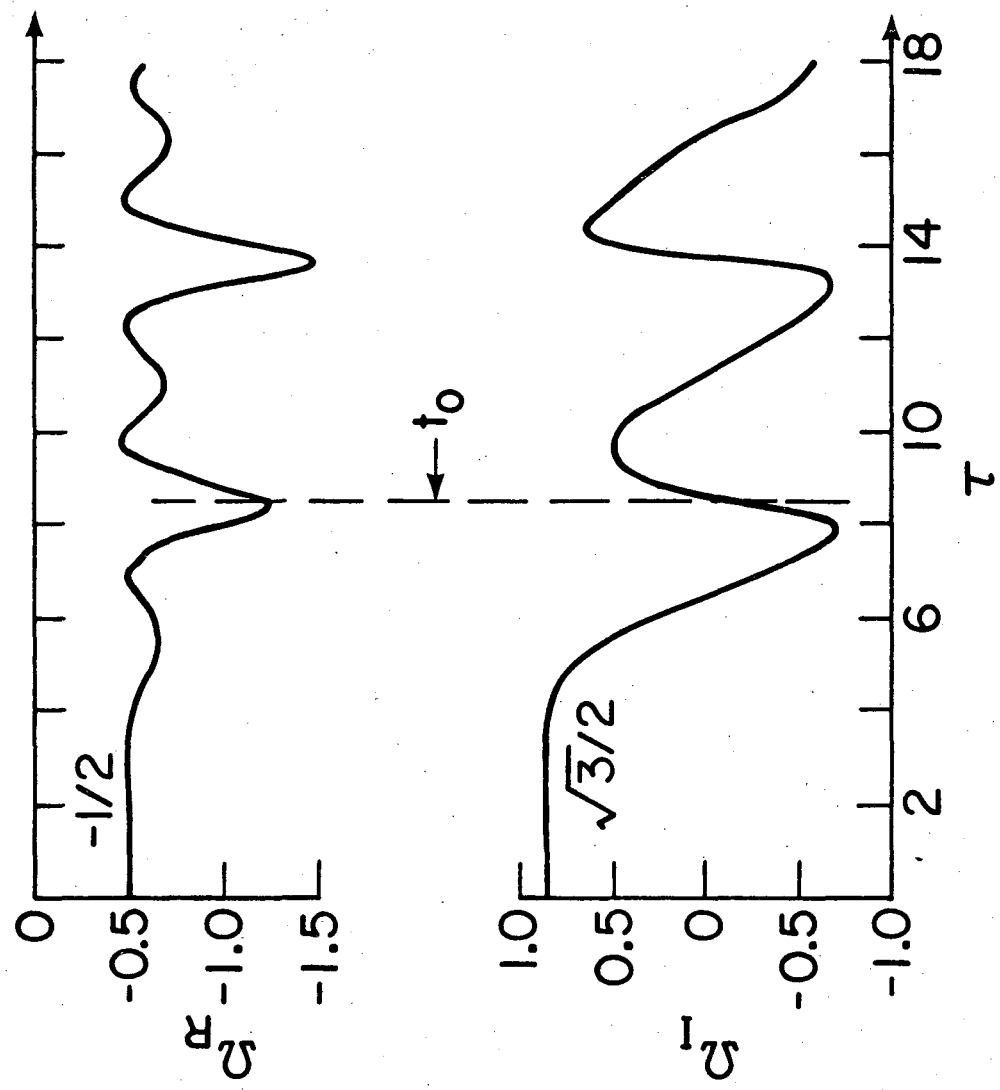
Fig. 7. Plots of the explicit functions  $\Omega_R(\tau)$  and  $\Omega_I(\tau)$  obtained from linearization of the reduced problem equations of motion, for the same values of free parameters as used in the numerical integration of Fig. 5.

Fig. 8. Same as Fig. 7, but for a nonzero bar length,  $\bar{\xi} = 1$ . (This figure bears the same relation to Fig. 6 as Fig. 7 does to Fig. 5.)

00004801796

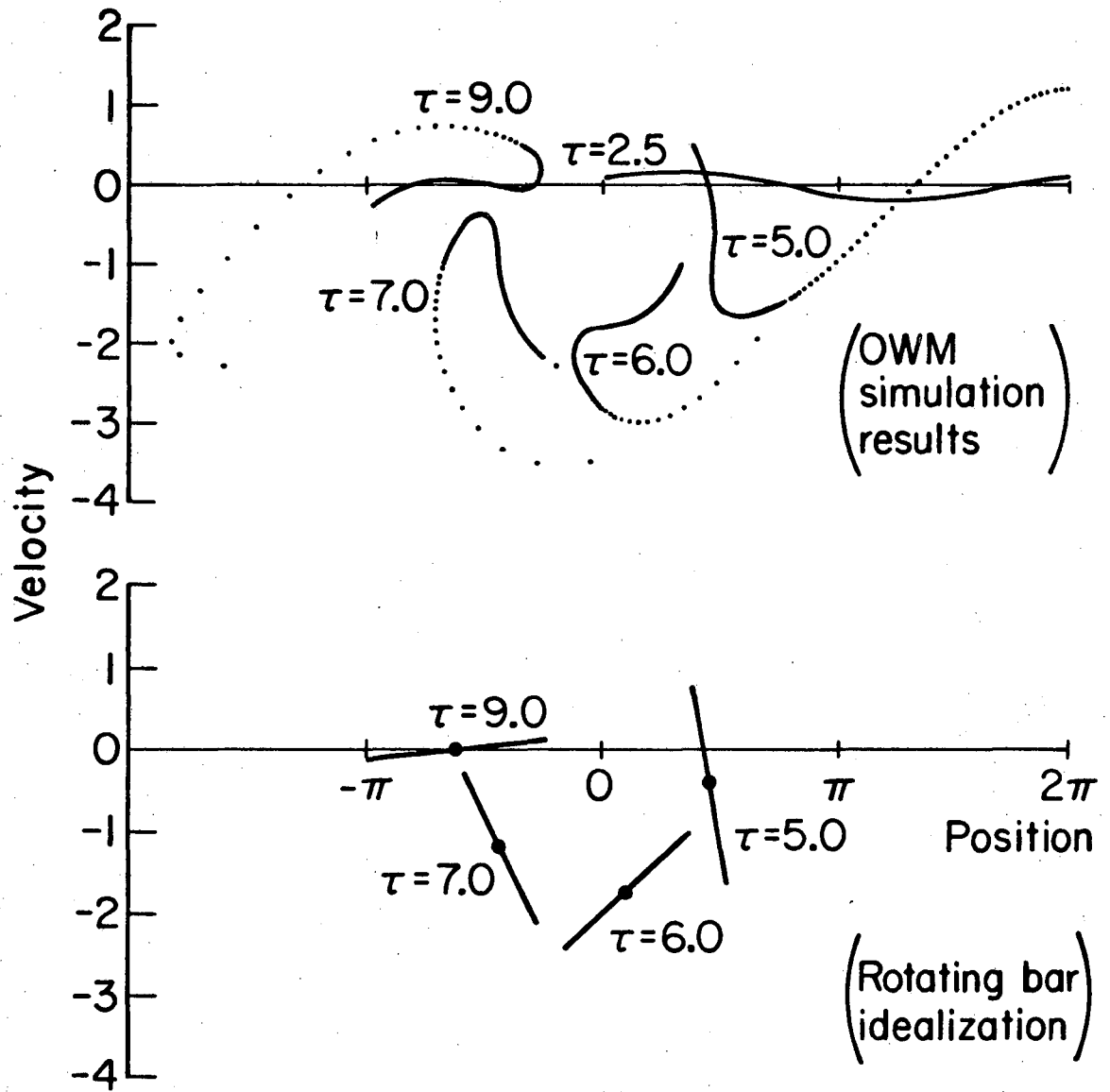


00004801797



XBL773-469

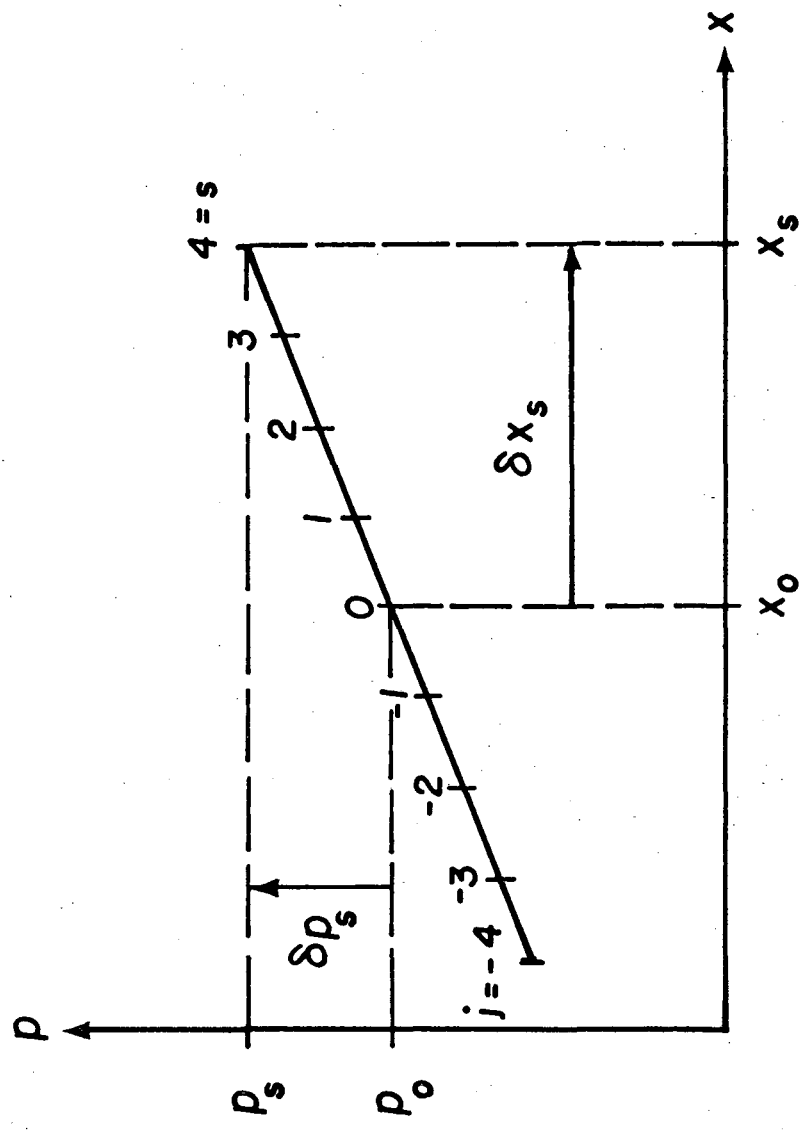
Fig. 1



XBL773-470

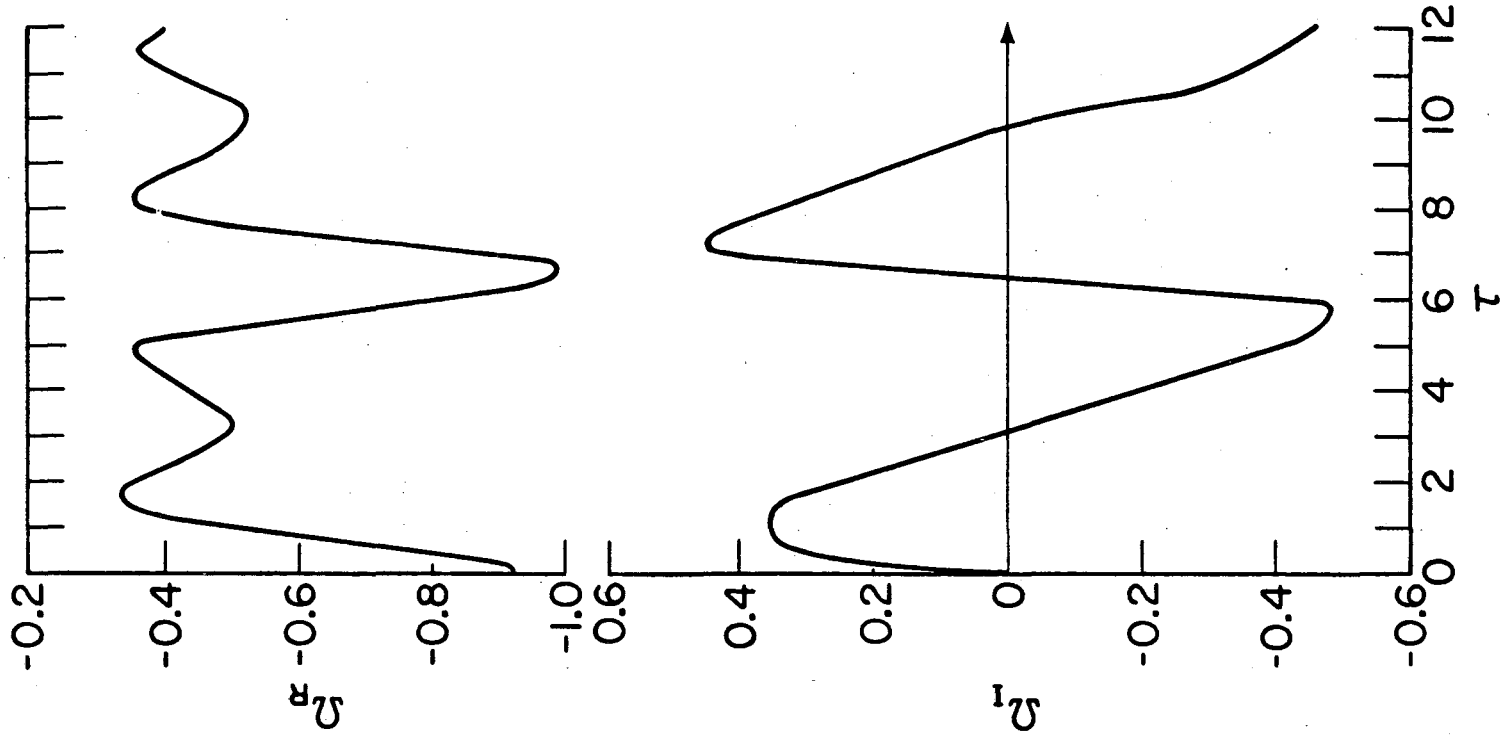
Fig. 2

00004801798



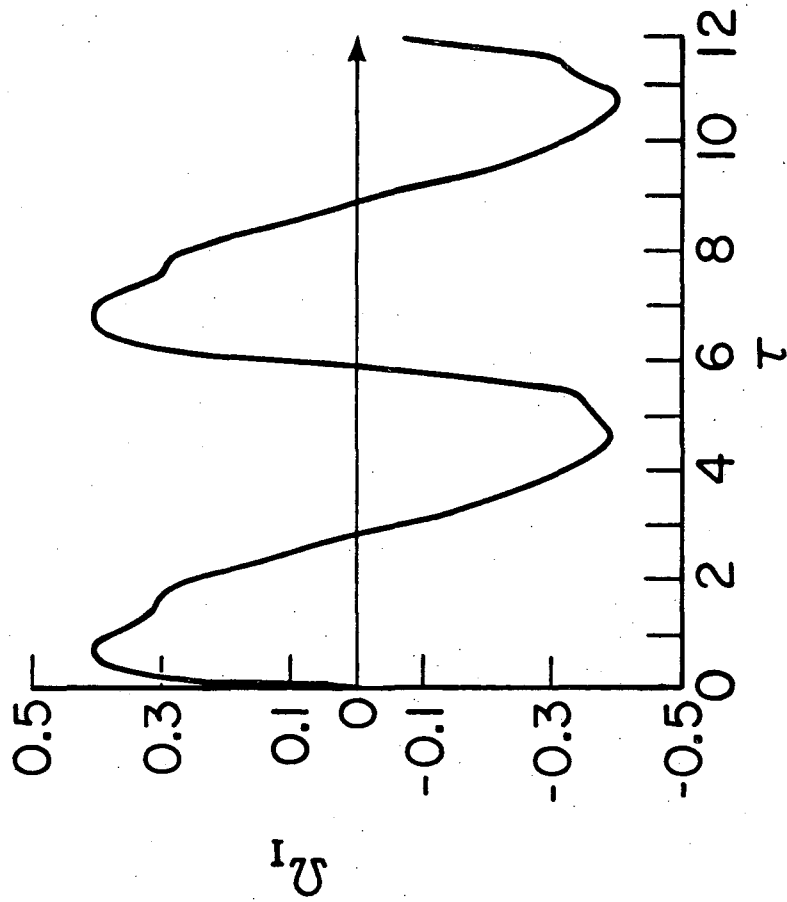
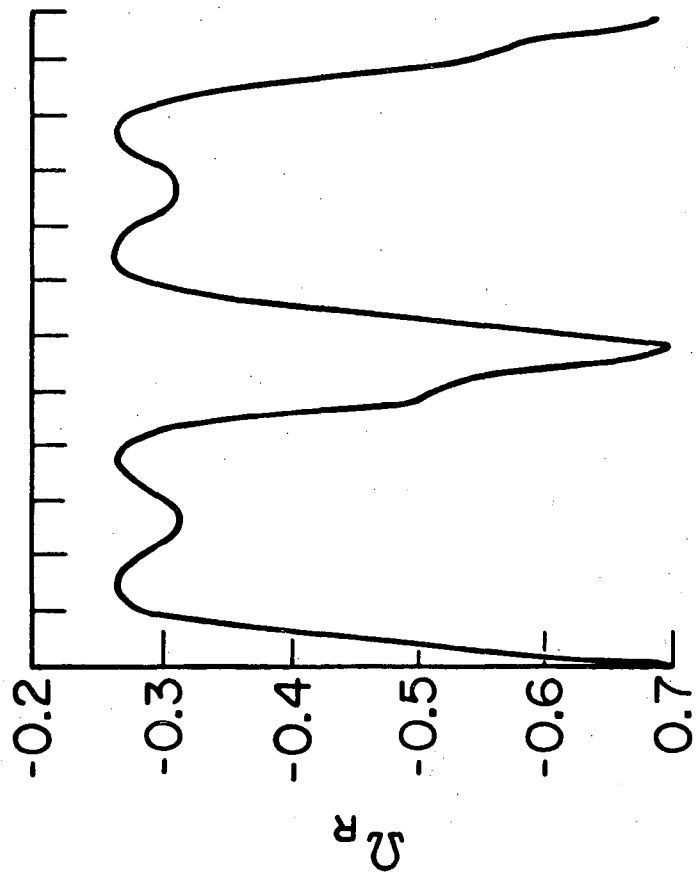
XBL 774-880

Fig. 3



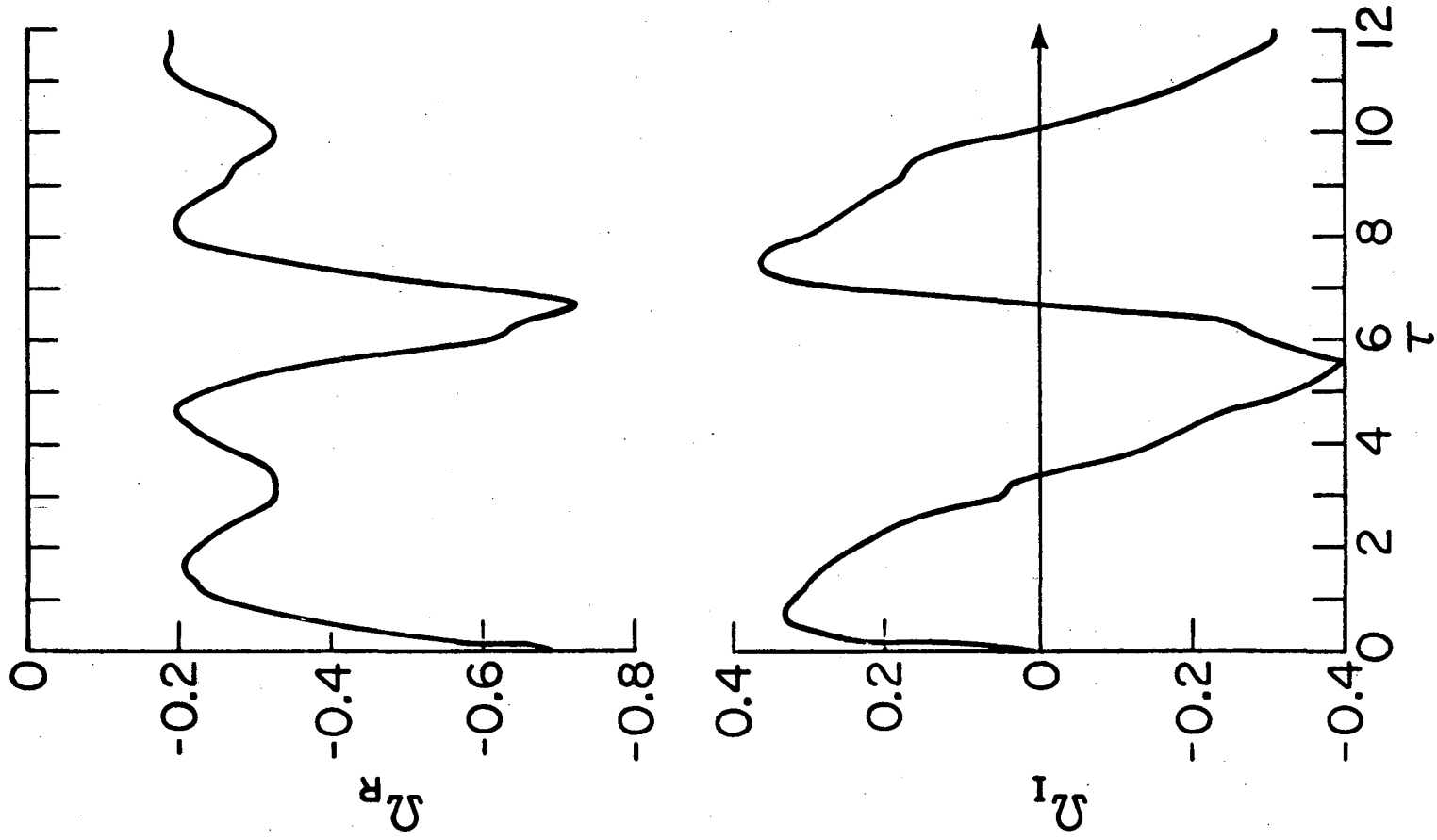
XBL773-471

Fig. 4



XBL773-473

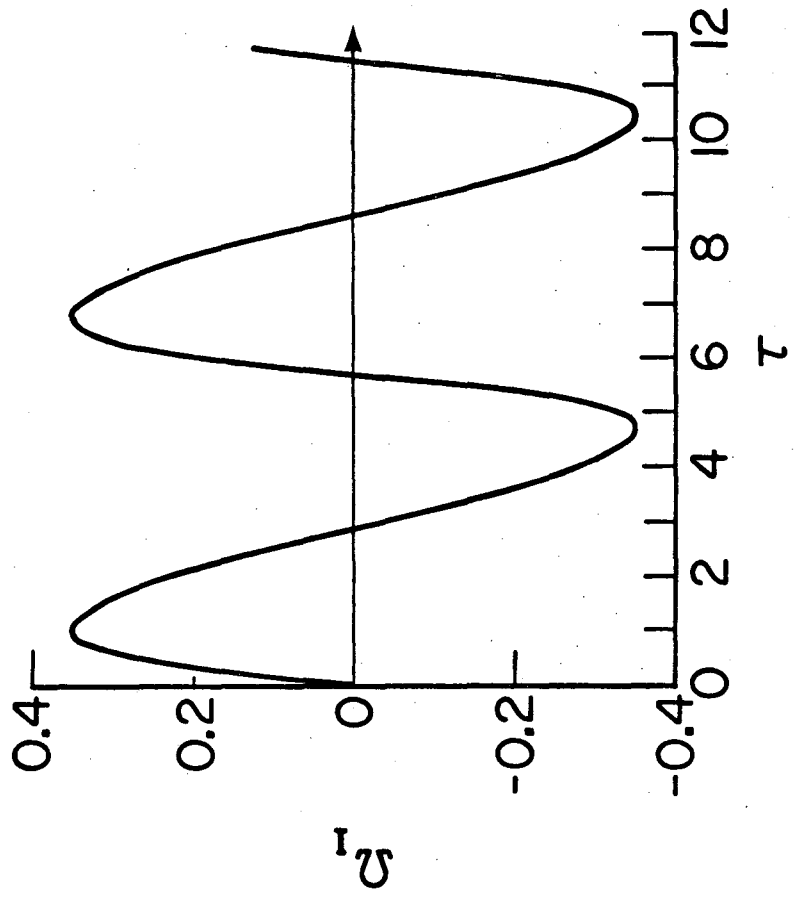
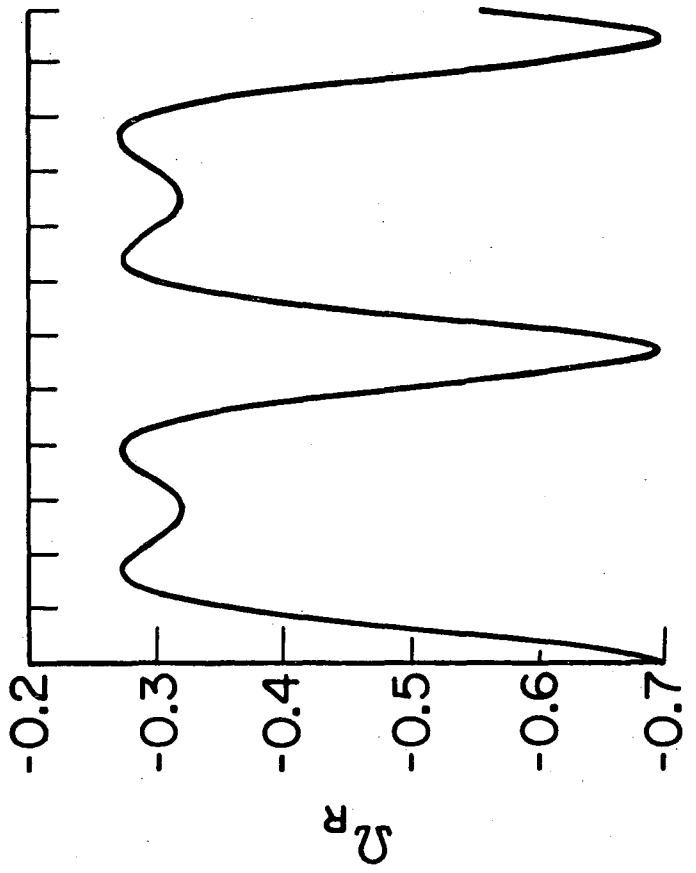
Fig. 5



XBL 773-472

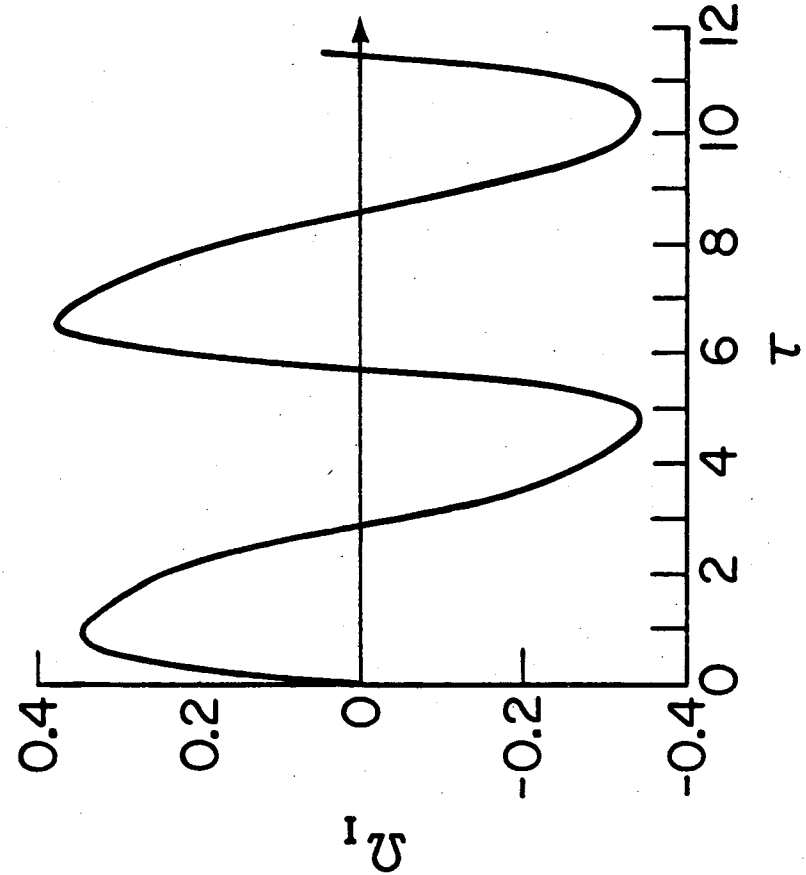
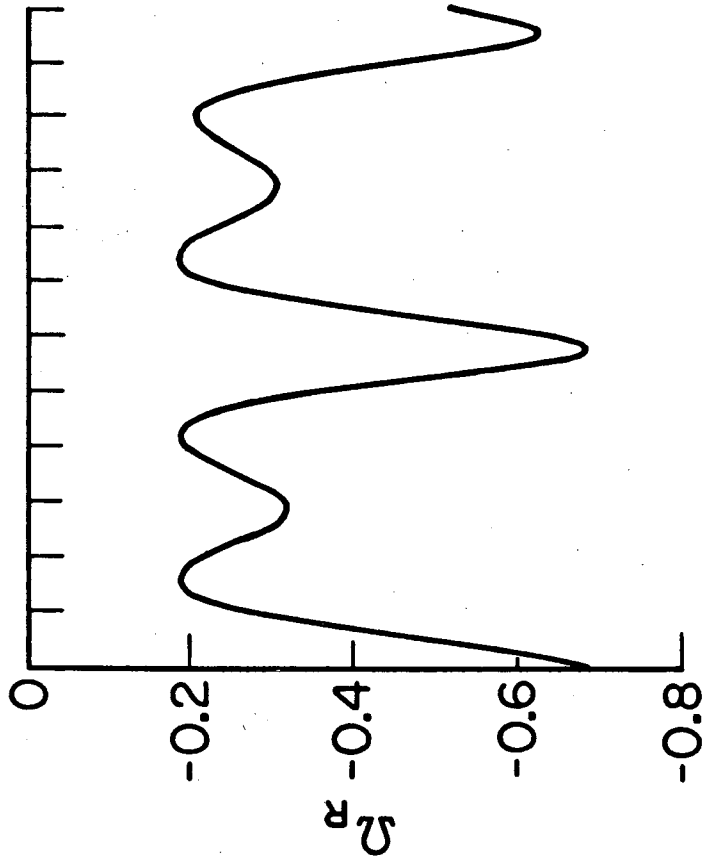
Fig. 6

00004801799



XBL 773-474

Fig. 7



XBL773-475

Fig. 8



0.0 4 8 0 1 3 0 0

This report was done with support from the Department of Energy. Any conclusions or opinions expressed in this report represent solely those of the author(s) and not necessarily those of The Regents of the University of California, the Lawrence Berkeley Laboratory or the Department of Energy.

TECHNICAL INFORMATION DEPARTMENT  
LAWRENCE BERKELEY LABORATORY  
UNIVERSITY OF CALIFORNIA  
BERKELEY, CALIFORNIA 94720